Research Article

Unmanned Aerial Vehicles for Photogrammetry: Analysis of Orthophoto Images over the Territory of Lithuania

J. Suziedelyte Visockiene,[1] R. Puziene,[1,2] A. Stanionis,[1] and E. Tumeliene[1]

[1]*Department of Geodesy and Cadastre, Vilnius Gediminas Technical University, Sauletekio Avenue 11, LT-10223 Vilnius, Lithuania*
[2]*Institute of Land Management and Geomatics, Faculty of Water and Land Management, Aleksandras Stulginskis University, Studentu 11, Akademija, LT-53361 Kaunas District Municipality, Lithuania*

Correspondence should be addressed to R. Puziene; ruta.puziene@vgtu.lt

It has been recently observed that aircrafts tend to be replaced by light, simple structure unmanned aerial vehicles (UAV) or mini unmanned aerial vehicles (MUAV) with the purpose of updating the field of aerial photogrammetry. The built-in digital photo camera takes images of the Earth's surface. To satisfy the photogrammetric requirements of the photographic images, it is necessary to carry out the terrestrial project planning of the flight path before the flight, to select the appropriate flying height, the time for acquiring images, the speed of the UAV, and other parameters. The paper presents the results of project calculations concerning the UAV flights and the analysis of the terrestrial images acquired during the field-testing flights. The experience carried out so far in the Lithuanian landscape is shown. The taken images have been processed by PhotoMod photogrammetric system. The paper presents the results of calculation of the project values of the UAV flights taking the images by digital camera Canon S100 and the analysis of the possibilities of the UAV orthophoto images' mode.

1. Introduction

Mapping of the terrain is a long lasting process that may last from half a year up to some years. Low altitude unmanned vehicles have already been started to be used to obtain high resolution aerial images, which has developed into the separate industry [1, 2]. A low altitude system flies underneath (up to 150 m) the air traffic [3]. UAV can be used for a flight. For this purpose, when meteorological conditions allow ground visibility, this kind of system is described by the term of unmanned aerial vehicle [4, 5]. A new and original technology that has been recently designed and constructed by the scientists and engineers of Space Science and Technology Institute (SSTI) together with the students of A. Gustaitis Aviation Institute (AGAI) should assist in developing that process. UAV are recommended for minor terrain mapping for the purposes of updating the maps, for military purposes, while exploring the nature and in other cases [5, 6].

The UAV may be of various sizes, shapes, and structures (miniature unmanned helicopter, rotary-wing UAV, quadracopter, drone, etc.) [7, 8]; and they are qualified by their manifold characteristics [9]. Previously, they were ordinary aircrafts under remote control, but recently autonomous UAV have been started to be used. Modern UAV move according to the preprogrammed flight pathway or they can be operated with the help of a more complicated system of dynamic automation. A digital, calibrated, and integrated camera is installed in an UAV, the purpose of which is to acquire the Earth's surface photographic images. The images made during the UAV flights can be investigated and processed by applying the methods of photogrammetry, with substantially lower costs to be incurred than they used to be in cases, when the images were taken from an airplane equipped with the complicated and rather expensive equipment, devices, and facilities [10–16].

The main photogrammetric workflow project stages with UAV are listed below:

(i) photogrammetric project parameters;

(ii) flight project;

(iii) quality of the images;

FIGURE 1: UAV constructed by SSTI and AGAI.

TABLE 1: Parameters of photo lens optics, camera Canon S100.

Calibration parameters	Result in pixels	Accuracy of the results
c_k	288.23	1.99
sxy	1.00	0.00
xh	−16.33	1.17
yh	−1.88	0.26
$A1$	-5.17×10^{-9}	7.17×10^{-11}
$A2$	1.89×10^{-16}	1.32×10^{-17}
$B1$	-3.90×10^{-7}	3.60×10^{-8}

(iv) image processing by photogrammetric or other special software;

(v) orthophoto image generalization and application of the acquired data.

The paper describes the stages of the workflow affecting the quality of the results of the photogrammetry operations.

2. Photogrammetric Project Parameters and Flight Planning with UAV Participation

The parameters of the photogrammetric project are the following:

(i) boundaries/borders of the photographed area;

(ii) model of the camera and its parameters;

(iii) expected scale of photographic images;

(iv) longitudinal and transversal overlapping of photographs;

(v) flight direction;

(vi) flight speed;

(vii) flight height;

(viii) data coordinate system.

The UAV operational time determines the dimensions of the photographed area boundaries/borders; the latter depend on the type of the installed motor. The UAV used for the research flights had an installed electric motor, 3.5 kg weight (see Figure 1).

This UAV (Figure 1) is able to cover 35–52 km during one flight; the maximum speed of the flight is 70 km/h or 19 m/sec and the flight time is 30–45 min (1.14 km/min).

The new UAV, constructed with the assistance of SSTI and AGAI institutions, had an installed CanonS100digital camera that was intended for test flights. The camera lens optics was calibrated with the help of the special German program Tcc according to the calibration stand, cube [14, 17, 18]. The following distortion parameters of the camera were determined: c_k: the distance of the focal length; sxy: the coefficient of the image scale; xh: the correction of the main image point x_0 of the coordinate X; yh: the correction of the

main image point y_0 of the coordinate Y; $A1$, $A2$: a camera lens radial-symmetric distortion; $B1$: a camera lens radial-asymmetric distortion. The obtained results are presented in Table 1. The camera lens radial-symmetric and radial-asymmetric distortions have small values.

The accuracy of the camera calibration is characterized by the standardized deflection (δ_0) of the weight unit, which indicates the accuracy of the identification and measurement of the points on the calibration stand. Theoretically, this value does not have to exceed 15 μm. After the calibration of camera Canon S100, the standard deflection of the weight unit was 3.16 μm; the acquired result is very good and acceptable.

The camera Canon S100 produces a 12.1-megapixel format (3000 × 4000 pixels) image. The sensor size of the digital matrix is 7.44 × 5.58 mm; thus, the smallest size of the image point (pitch of the pixel) is 1.86 um. The calibrated distance of the focal length is c_k = 5.361 mm (Table 1). A small distance of the focal length indicates that this camera has a wide field of view; therefore a large area of the location can be covered when taking images with this camera.

The distance of the camera focal length and the flight height of the UAV determine the scale size of the image. The traditional calculation formula of the photogrammetric image scale is the following [19]:

$$M_b = 1 : m_b = \frac{c_k}{h_g}, \tag{1}$$

here m_b is an image scale denominator; c_k is the distance of the focal length; h_g is the flight height of the UAV.

These values have to be considered and calculated when planning the UAV flight. The correct flight planning has influence on the accuracy and volume of the collected information about the desired regions [8, 20]. The theoretical planning of the UAV flight is justified by the calculation of the arrangements of the images along the flight route [8, 21]. The scheme of the flight project is given in Figure 2.

In Figure 2, d is the size of the image; p is the longitudinal overlapping of the adjacent images on the flight route; b is the base for taking images (the distance between the adjacent centers of the images); q is a transverse overlapping of the images between the upper and lower flight routes.

The image size d depends on the camera expression. During the research flights the camera Canon S100 was used; the maximum expression of the camera was 12.1 MP. The image of 4000 × 3000 pixels was acquired (7.44 × 5.58 mm). One has to know the size of the image when calculating

Table 2: Flight project values, with camera Canon S100.

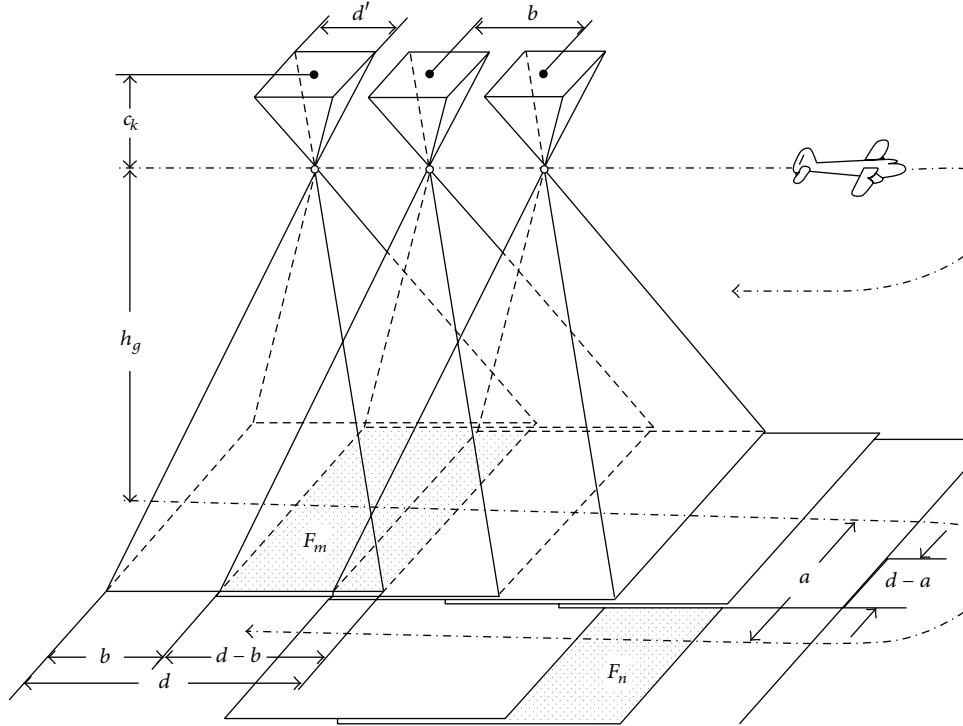| $1:m_b$	h_g [m]	d, [m]	b ($p = 70\%$), [m]	a ($q = 45\%$), [m]	a ($q = 60\%$), [m]
1 : 2000	107	149×112	45	61	45
1 : 2500	134	186×140	56	77	56
1 : 3000	161	223×167	67	92	67
1 : 3500	188	260×195	78	107	78
1 : 4000	214	298×223	89	123	89
1 : 4500	241	335×251	100	138	100
1 : 5000	268	372×279	112	153	112
1 : 5500	295	409×307	123	168	123

Figure 2: Flight project scheme.

the longitudinal and transversal overlapping of the images during the flight. The formula for the calculation is

$$p = \frac{d - b}{d} \times 100,$$
$$q = \frac{d - a}{d} \times 100, \tag{2}$$

where a is the distance between the adjacent flights calculated according to this formula:

$$a = d \times \left(1 - \frac{q}{100} \right). \tag{3}$$

The project values of the UAV flights were calculated according to formulae (1)–(3); images were taken by the camera Canon S100 and under ideal flight conditions. The obtained results are given in Table 2.

The flight project values (Table 2) are required in order that not a single area of the investigated area is left without being captured, between the adjacent images and routes, during the process of the UAV flight and taking images of the determined area. When selecting the photogrammetric project parameters it is necessary to take into consideration certain weather conditions that occur during the flight and especially the wind direction. The flow of the air causes the wind speed to increase with increasing height above the ground. The wind blows along the negative direction of z-axis, the positive y-axis points to the sky, and the direction of x-axis is dependent on right-handed rule [22]. The relation between wind speed and height above the surface is described in the articles [23]. Also flight height can be obtained from Ground Sample Distance (GSD) or a pixel size in the terrain and depends on the camera focal length, camera sensor width, and the distance covered on the ground by one image. The GSD calculation formula is

$$\text{GSD} = \frac{\text{pix} \times h_g}{c_k}, \tag{4}$$

where pix is pitch of the pixel of the camera sensor; h_g is the flight height of the UAV; c_k is the distance of the camera focal length. If the UAV flight is high at 214 m above the ground and the camera's focal length is 1.86 um, the image resolution GSD will be 7.4 cm per pixel. The size on the ground will be 3000×0.074 m = 222 m by 4000×0.074 m = 296 m. UAV is oriented so that the 296 m axis is parallel to in-track and 222 m axis is along the cross-track direction. We recommend in-track (flight direction) overlap, 70% (Table 2), and the flight speed 19 m/sec. UAV moves 89 m relative to the ground (70% of 296 m = 207 m; 296 − 207 m = 89 m) and takes a photo. If the flight speed is 19 m/sec, you need to take a photo every 5 sec. We recommend at least 45% cross-track overlap. The spaces between the above UAV flight lines should not be greater than 123 m. Tighter flight lines are good.

Each UAV has its certain flight speed and direction. There are eight possible flight directions (north, northeast, east, southeast, south, southwest, west, and northwest). Also each UAV has three possible orientations, such as turning left, going straight, and turning right [24]. The traditional recommended photogrammetry flight direction is east-west or north-south [1]. The images taken while keeping to the mentioned above flight directions are easy to process by the photogrammetric method. However, if needed, the direction is possible to be changed.

The flight speed depends on wind speed. The allowable wind speed-limit classification for UAV is shown in [25]. The UAV gets Earth-wise speed from GPS (Global Point System). In order to calculate wind velocity vector inertial Cartesian coordinate system-wise, additional information on UAV position in space is being taken into account. The authors of the article have presented the calculated track of wind speed during the year [26]. In autumn wind speed keeps increasing each month: average wind speed in September is 4.5–5.0 m/s and in November is 3.5–6.5 m/s. Differences range of the wind speed at the seaside and in Eastern country regions is about 2 m/s. In winter wind speed increases slowly: at the seaside average wind speed ranges from 5.5 m/s to 8.0 m/s, and in the Eastern country regions it ranges from 5.0 m/s to 5.5 m/s. The difference is about 2.5–3.0 m/s. In spring wind speed decreases: at the seaside it ranges between 5.0–5.5 m/s and 4.5–5.0 m/s, in other regions it is from 4.0 m/s to 3.5 m/s, and in summer wind speed at the seaside is 4.0–5.0 m/s, while in Eastern regions it is 2.5–4.0 m/s [26].

UAV flight height depends on nebulosity and fog. The authors of the article have also included the diagram of fog formation in Kaunas and Siauliai aerodromes each month throughout the year [26]. It has been found that the average number of foggy days in Kaunas aerodrome in September, October, and November exceeded 5 days; in Siauliai aerodrome the average number of foggy days also exceeded 5 days. Consequently, the most favorable period of the year for the UAV flights is between April and August, when wind speed decreases and there are less foggy days.

Based on the parameters of the photogrammetric project and on the values of the flight project (Table 2), the UAV flight could be marked using the software (Mission Planner) during the flight or previously, when indicating the initial and final points of the planned flight route on the Google Earth map. Thus, on the screen or, to be more exact, on the tables of the software, the beginning and end of the geodetic coordinate points of the route, longitude and latitude, appear. During the process of acquiring images, the coordinates of the image centers GPS, which later could be applied for the photogrammetric measurements of the images, are fixed.

Figure 3: Flight configurations in Kirtimai.

3. The Analysis of the Area Views Taken from UAV

The images of the area taken from UAV are used [5]:

   (i) to compile orthophoto images of the area;

  (ii) to compile and update a topographic and cadastral map of the area;

 (iii) for the forest management needs and requirements;

 (iv) to compile the surface model and to carry out measurements;

  (v) for military purposes;

 (vi) to observe the surrounding vegetation;

(vii) to observe the power supply network conditions;

(viii) in the architecture;

 (ix) and so forth.

Many researches work on designing of software for using of UAV image processing [8, 27, 28]. There are some of their examples: PhotoMod (Russia), Pix4d mapper (Switzerland), Photo Scanner (Russia), and so forth. The software design and engineering play a great role in the life cycle of training simulators. Electronic, information engineering, and aeronautic sciences develop and create new mathematical models and software for photogrammetry purpose [29, 30]. The test project has been made by PhotoMod Lite modular photogrammetric system.

Kirtimai area (Vilnius region), dated 2012-10-09, is one of the examples of the photogrammetric processing of the area images, taken from UAV. The view of the flight route is presented in Figure 3.

The photogrammetric calculations were made according to 6 images of the area (see Figure 4), which were corrected due to the camera lens distortions (see Table 1).
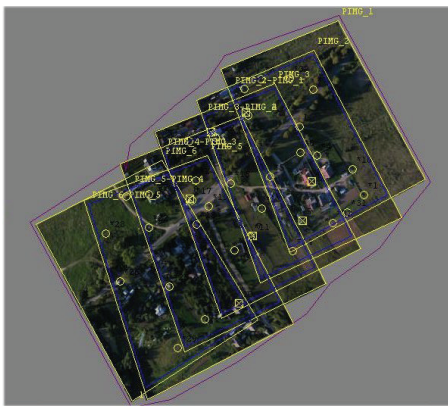
FIGURE 4: Images IMG_3, 4, 5.

FIGURE 5: Geometric model of the area.

FIGURE 6: Topographic data of the area.

FIGURE 7: Orthophoto image of the area.

The geometric model for one route in the territory of Kirtimai was compiled with the help of the photogrammetric system PhotoMod according to the tie points and ground control points, selected on the images, the rectangular coordinates of which were determined on the orthophoto images (Figure 5) in 2009 on the website http://www.geoportal.lt/.

The geometric model of the area made by the photogrammetric method is considered to be the basis of the data collecting for the orthophoto image, for the vector type-topographic, and for the 3D or three-dimensional spatial data. Based on the geometric model of Kirtimai territory (see Figure 5), basic data of the topographic map of the area were collected by the stereo digital method (see Figure 6) and the orthophoto image (see Figure 7) was generated.

It is possible to make observations of the area on the orthophoto image or analyze the visible modifications in nature and occurring economic changes, by comparing the available information about the present field conditions on the site with the possessed latest cartographic material [31]. The situation available on the orthophoto image of Kirtimai made in 2009 was juxtaposed with the view on the compiled Kirtimai orthophoto image (see Figure 7). The result is presented in Figure 8.
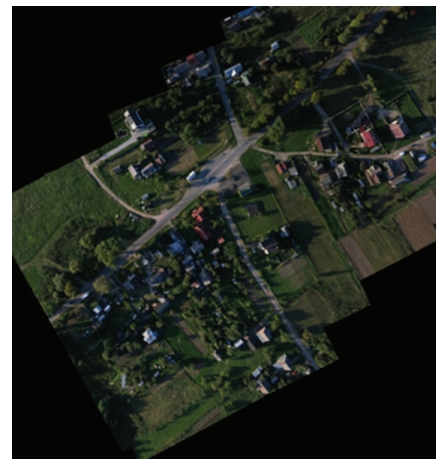
The orthophoto image made by UAV in 2012 is obviously brighter and more intense. The situation of the area has undergone the changes in the surrounding nature, the modifications in the vegetation due to the changes of the agricultural land usage, and the paving of the road. The area has changed insignificantly what concerns the construction of new buildings; no new farm has been built on the site.

(a)   (b)

FIGURE 8: Orthophoto images ((a) in 2009; (b) in 2012 compiled by the authors).

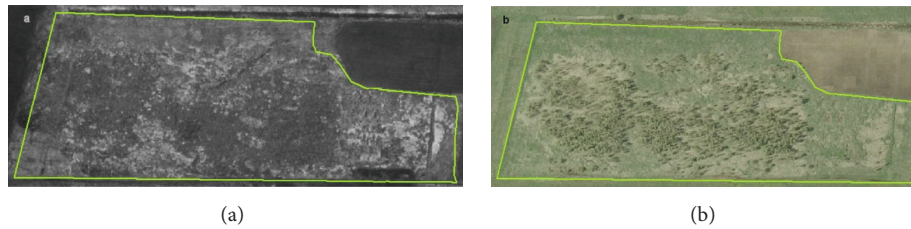(a)   (b)

FIGURE 9: (a) The abundant, unused agricultural field in 1995 on the orthophoto image; (b) the same field in 2009 on the orthophoto image, but with the forest undergrowth.

(a)   (b)

FIGURE 10: (a) Mature forest in 1995 on the orthophoto image, (b) the orthophoto image in 2012: one part is deforested and the young stands are sown.

Majority of changes take place at the expense of agricultural land [32]. Recently, a large area of agricultural land has turned into the unbroken soil and at present is not used according to the purpose prescribed. The agricultural land located near the forests is going to overgrow by the shoddy bushes and forest undergrowth (Figure 9). It is rather complicated to renew the agricultural activities on the former agricultural territories, and, in case of the infertile soil, it is inappropriate and expensive.

Concerning woodlands, changes are rather noticeable on the orthophoto image. Forest undergrowth (see Figure 10) has turned into the mature forest. At present, the orthophoto images are widely used by foresters when compiling the database of the Geographic Information Systems (GIS), for the purposes of collecting data on the forest taxation, for determining the composition of the forest species and for detecting the forest areas damaged by diseases, for allocating forest areas for lumbering purposes, and so forth.

FIGURE 11: Arable land with boggy areas.

The images of some separate flights captured the deteriorations in the reclamation systems. In the areas, where the land reclamation facilities have been poorly functioning, the soaked agricultural field areas or the pits were noticed (Figure 11). These soils usually tend to be marshy over a long period or overgrow by bushes and weeds or become the abandoned and unusable land.

The new AGAI and SSTI technology can serve as a means for simple and quick updating of the databases of the digital maps after the substantial changes in the terrain of the investigated area.

With the assistance of the photogrammetric system function *Envi Ex* "*Feature Extraction*," it is possible to perform the automatic identification of the target object on the available image or on the orthophoto image (Figure 12).

The program fixates the targets automatically and then it registers them onto the separate data layer. Later, the information is possible to be analyzed and processed.

According to the data of the orthophoto image, it is possible to observe the vegetation of the plants. The interpretation view of the vegetation mapping is compiled by means of Envi Ex program function "Vegetation Suppression" (Figure 13). According to the tone of the view colour, it is possible to judge the state of the plants' growth during the diverse periods of their growing, to compile the diagrams of the observations of vegetation and calculate the index of vegetation.

From the economic point of view, it is very important to conduct systematic observations concerning the state of the crops and to forecast their fertility. The remote study method applied for the crop investigation is based on the difference of optical characteristics of the crop. The electromagnetic wave length interval of the Sun rays' spectral composition, reflected from the plants, is 0.4–2.5 um. It depends on the radiation absorption, which depends on the amount of chlorophyll within the visible zone of waves; for water it is in the middle spectrum zone of the infrared waves, as well as on the histological peculiarities of the leaves. In the visible spectral zone, plants assimilate the radiation energy most intensively in blue, red, and green spectrum zones. It depends on the structure of plant leaves. Transformations of the coefficient curve of the spectral brightness are caused by the dynamics of the plants phenology, the changes, preconditioned by the deficiency of water, nutrients, and increased salinity of the soil [32, 33]. If the parameters of the multizone image system are selected correctly, as well as the time of probing, it is possible to determine the species of the plants and their state. These observations are performed with the spectral images taken from the UAV, designed and constructed at SSTI (Figure 13).

Special climatic conditions, especially fogs and clouds, prevent acquiring high quality satellite images in the territory of Lithuania. The analysis of the information on Lithuanian METAR aerodromes has been performed by the scientist Borkovskij [26]. It has been found that the tendency of worse visibility conditions increase in Lithuanian international airports appears in September, October, November, December, January, February, and March. After carrying out the meteorological studies, it has been determined that the majority of the sunny days in the territory of Lithuania are in April–August months [25, 26]. During that period, the greatest probability of taking valid multispectral images that may be used for the analysis and cartographic operations exists. These disturbances are not relevant to the UAV operations, the flight height of which is 300 m. The flights could be made in any month and in case the image quality is poor, it is possible to repeat the flight, causing no extra money and time.

4. Conclusions

(a) In order to avoid missing any not captured area, it is necessary to work out the flight route project before the start of unmanned aerial vehicle (UAV) flight, if the objective of the flight is the compiling of the map. The weather conditions have to be taken into account when planning the workflow of the future flight.

(b) The terrain orthophoto images can be used for the analysis of the environment modifications and economical changes of the area, when comparing the information collected under the field conditions on a certain locality with the acquired latest cartographic material.

(c) At present, the orthophoto images are widely applied in compiling the Geographic Information Systems (GIS) databases for foresters, for collecting data on forest taxation, for determining forest species status and areas damaged by diseases, for planning the lumbering of the forest, and so forth.

(d) It is possible to observe the vegetation of plants on the spectral images and on the orthophoto image.

(e) It is possible to use the images taken by UAV for military purposes, for the analysis of the targets on the area.

(f) The new technology constructed by SSTI and AGAI may be used as a simple and fast way to update the digital map databases after substantial modifications of the area.
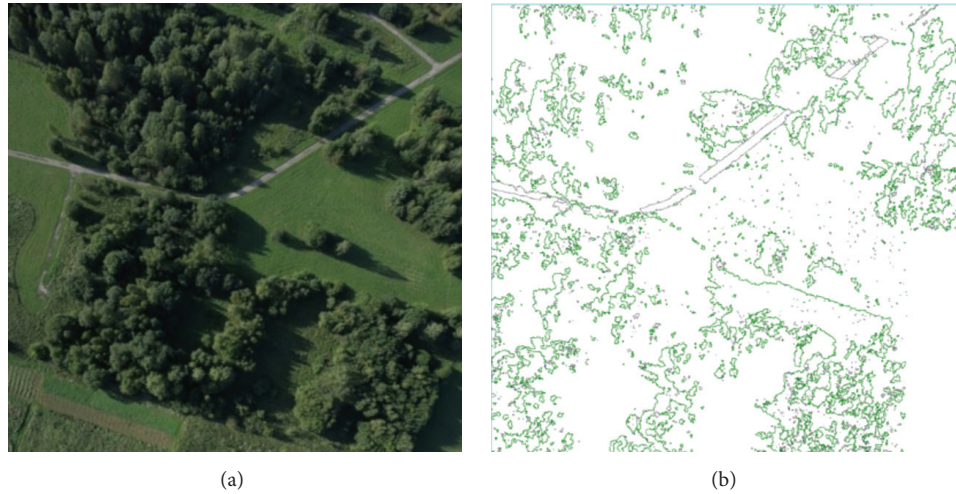
(a)

(b)

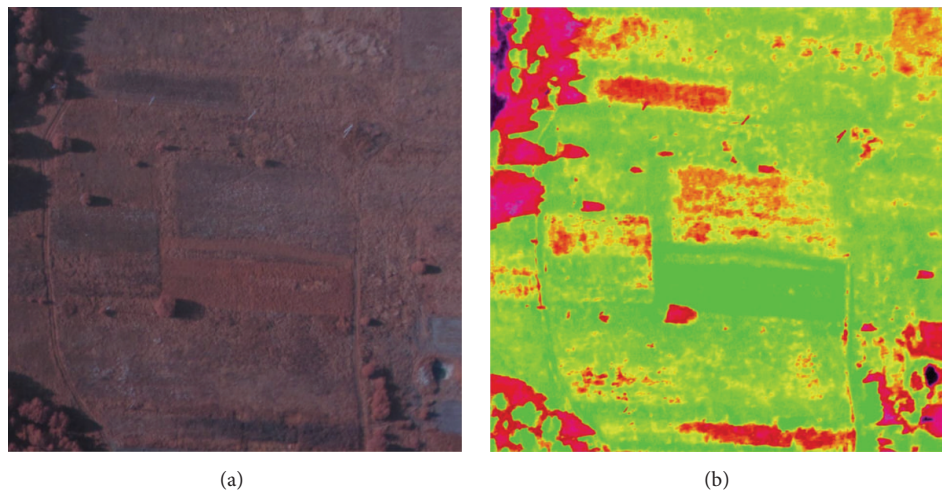FIGURE 12: Automatic fixation of the target by Envi Ex program.

(a)

(b)

FIGURE 13: Images for plants observation: (a) a spectral image; (b) the compiled colour images for vegetation state observations.

(g) The climatic conditions, especially clouds and fogs, prevent acquiring high quality satellite images on the territory of Lithuania. UAV flights may be planned to be accomplished during the period of April–August; also they may be conducted during the rest of the year, if the weather conditions are favorable. These disturbances are not significant for an unmanned aerial vehicle, the flight height of which is up to 300 m.

Conflict of Interests

The authors declare that there is no conflict of interests regarding the publication of this paper.

Acknowledgment

References

[1] G. Cho, A. Hildebrand, J. Claussen, P. Cosyn, and S. Morris, "Pilotless aerial vehicle systems: size, scale and functions," *Coordinates*, vol. 9, no. 1, pp. 8–16, 2013.

[2] G. Petrie, "Commercial operation of lightweight UAVs for aerial imaging and mapping," *GEOInformatics*, vol. 16, no. 1, pp. 28–39, 2013.

[3] J. Everaerts, "The use of unmanned aerial vehicles (UAVs) for remote sensing and mapping," *The International Archives of the Photogrammetry, Remote Sensing and Spatial Information Sciences (ISPRS Archives)*, vol. 37, no. 1, pp. 1187–1191, 2008.

[4] I. Colomina and P. Molina, "Unmanned aerial systems for photogrammetry and remote sensing: a review," *ISPRS Journal of Photogrammetry and Remote Sensing*, vol. 92, pp. 79–97, 2014.

[5] L. Ding, H. Wu, and Y. Yao, "Chaotic artificial bee colony algorithm for system identification of a small-scale unmanned helicopter," *International Journal of Aerospace Engineering*, vol. 2015, Article ID 801874, 11 pages, 2015.

[6] A. Eltner and D. Schneider, "Analysis of different methods for 3D reconstruction of natural surfaces from parallel—axes UAV images," *The Photogrammetric Record*, vol. 30, no. 151, pp. 279–299, 2015.

[7] Y. Xu, W. Sun, and P. Li, "A miniature integrated navigation system for rotary-wing unmanned aerial vehicles," *International Journal of Aerospace Engineering*, vol. 2014, Article ID 748940, 13 pages, 2014.

[8] S. Tang, X. Lu, and Z. Zheng, "Platform and state estimation design of a small-scale UAV helicopter system," *International Journal of Aerospace Engineering*, vol. 2013, Article ID 524856, 13 pages, 2013.

[9] A. S. Laliberte, J. E. Herrick, A. Rango, and C. Winters, "Acquisition, orthorectification, and object-based classification of unmanned aerial vehicle (UAV) imagery for rangeland monitoring," *Photogrammetric Engineering & Remote Sensing*, vol. 76, no. 6, pp. 661–672, 2010.

[10] H. Eisenbeiss, "A Mini Unmanned Aerial Vehicle (UAV): system overview and image acquisition," in *Proceedings of the International Workshop on Processing And Visualization Using High-Resolution Imagery: International Archives of Photogrammetry, Remote Sensing and Spatial Information Sciences*, vol. 36-5/W1, Pitsanulok, Thailand, November 2004.

[11] U. Niethammer, S. Rothmund, M. R. James, J. Travelletti, and M. Joswig, "UAV-based remote sensing of landslides," *International Archives of the Photogrammetry, Remote Sensing and Spatial Information Sciences*, vol. 38, pp. 496–501, 2010, Part 5 Commission V Symposium.

[12] F. Chiabrando, F. Nex, D. Piatti, and F. Rinaudo, "UAV and PRV systems for photogrammetric surveys in archaeological areas: two tests in the Piedmont region (Italy)," *Journal of Archaeological Science*, vol. 38, no. 3, pp. 697–710, 2011.

[13] K. Choi and I. Lee, "A UAV based close-range rapid aerial monitoring system for emergency responses," *International Archives of the Photogrammetry, Remote Sensing and Spatial Information Sciences*, vol. 38-1/C22, pp. 247–252, 2011.

[14] M. Yun, J. Kim, D. Seo, J. Lee, and C. Choi, "Application possibility of smartphone as payload for photogrammetric UAV system," in *Proceedings of the International Archives of the Photogrammetry, Remote Sensing and Spatial Information Sciences, XXII ISPRS Congress*, vol. XXXIX-B4, pp. 349–352, Melbourne, Australia, August-September 2012.

[15] J. Kim, S. Lee, H. Ahn, D. Seo, S. Park, and C. Choi, "Feasibility of employing a smartphone as the payload in a photogrammetric UAV system," *ISPRS Journal of Photogrammetry and Remote Sensing*, vol. 79, pp. 1–18, 2013.

[16] M. Pérez, F. Agüera, and F. Carvajal, "Low cost surveying using an unmanned aerial vehicle," *International Archives of the Photogrammetry, Remote Sensing and Spatial Information Sciences*, vol. 40-1/W2, pp. 311–315, 2013.

[17] J. Sužiedelytė-Visockienė and D. Bručas, "Influence of digital camera errors on the photogrammetric image processing," *Geodezija ir Kartografija*, vol. 35, no. 1, pp. 29–33, 2009.

[18] J. Sužiedelytė-Visockienė, "Photogrammetry requirements for digital camera calibration applying Tcc and MatLab software," *Geodesy and Cartography*, vol. 38, no. 3, pp. 106–110, 2012.

[19] J. Albertz and W. Kreiling, *Photogrammetric Guide*, Wichmann, Karsruhe, Germany, 4th edition, 1989.

[20] H. Ergezer and K. Leblebicioglu, "Path planning for UAVs for maximum information collection," *Journal of Intelligent & Robotic Systems*, vol. 73, pp. 737–762, 2014.

[21] P. Barry and R. Coakley, "Field accuracy test of RPAS photogrammetry," *International Archives of the Photogrammetry, Remote Sensing and Spatial Information Sciences*, vol. 40-1/W2, pp. 27–31, 2013.

[22] B. Zhu, Z. Hou, S. Shan, and X. Wang, "Equilibrium positions for UAV flight by dynamic soaring," *International Journal of Aerospace Engineering*, vol. 2015, Article ID 141906, 8 pages, 2015.

[23] P. P. Sukumar and M. S. Selig, "Dynamic soaring of sailplanes over open fields," *Journal of Aircraft*, vol. 50, no. 5, pp. 1420–1430, 2013.

[24] C. H. Ru, X. Qi, and X. Guan, "Distributed cooperative search control method of multiple UAVs for moving target," *International Journal of Aerospace Engineering*, vol. 2015, Article ID 317953, 12 pages, 2015.

[25] R. Kikutis and J. Stankūnas, "Survey of navigation algorithms and their use for the flights of unmanned aerial vehicles in windy conditions," *Aviation Technologies*, vol. 2, no. 2, pp. 63–68, 2014.

[26] D. Borkovskij, "Distribution of dangerous meteorological phenomena and their effects at aerodromes of international airports of Lithuania," *Aviation Technologies*, vol. 1, no. 2, pp. 62–66, 2013.

[27] G. Cai, B. M. Chen, T. H. Lee, and M. Dong, "Design and implementation of a hardware-in-the-loop simulation system for small-scale UAV helicopters," *Mechatronics*, vol. 19, no. 7, pp. 1057–1066, 2009.

[28] M. Dong, B. M. Chen, G. Cai, and K. Peng, "Development of a real-time onboard and ground station software system for a UAV helicopter," *Journal of Aerospace Computing, Information and Communication*, vol. 4, no. 8, pp. 933–955, 2007.

[29] A. AbdElHamid and P. Zong, "A novel software simulator model based on active hybrid architecture," *International Journal of Aerospace Engineering*, vol. 2015, Article ID 107301, 19 pages, 2015.

[30] J. Zhang, R. Wang, and L. Pan, "The system of lifetime prediction for VFD based on VB and MATLAB," in *Proceedings of the International Conference on Artificial Intelligence and Computational Intelligence (AICI '09)*, pp. 59–62, IEEE, Shanghai, China, November 2009.

[31] V. Kupkova, I. Bicik, and J. Najman, "Land cover changes along the iron curtain 1990–2006," *Geografie*, vol. 118, no. 2, pp. 95–115, 2013.

[32] J. Primicerio, S. F. Di Gennaro, E. Fiorillo et al., "A flexible unmanned aerial vehicle for precision agriculture," *Precision Agriculture*, vol. 13, no. 4, pp. 517–523, 2012.

[33] A. S. Laliberte, M. A. Goforth, C. M. Steele, and A. Rango, "Multispectral remote sensing from unmanned aircraft: image processing workflows and applications for rangeland environments," *Remote Sensing*, vol. 3, no. 11, pp. 2529–2551, 2011.